Dissociation Dynamics of CO_2 on Cu(110) Studied Over a Wide Range of Incident Energies

Saurabh Kumar Singh and Pranav R. Shirhatti*

Tata Institute of Fundamental Research, 36/P Gopanpally, Hyderabad 500046, Telangana, India

E-mail: pranavrs@tifrh.res.in

Phone: +91 040 20203061

Abstract

In this work, we have studied the dissociation dynamics of CO_2 on a Cu(110) surface using molecular beams with incidence energies ranging from 0.28 eV to 4.6 eV. The incident energy dependence of the initial dissociative reaction probabilities (S_0) of CO_2 showed two distinct characteristics. At first, S_0 exhibits a rapid increase from 1.8×10^{-4} at 0.28 eV to more than 150-fold at 2 eV. Beyond this, only a small increase by less than a factor of 1.5 was observed in the 2 eV to 4.6 eV range, with the S_0 being 4.1×10^{-2} at 4.6 eV. Incident angle-dependent measurements reveal total energy scaling to be followed. Measurements using a heated nozzle showed no observable enhancement in S_0 due to the vibrational energy of the incident molecules, with an upper limit of vibrational efficacy estimated to be 0.25. Furthermore, an increase in O-atom saturation coverage (resulting from CO_2 dissociation) from 0.5 ML to 0.66 ML was observed at high impact energies (> 3 eV), suggesting that newer dissociation sites become accessible at higher energies.

Introduction

Understanding the dissociation dynamics of small molecules on metal surfaces under well-controlled conditions is an important stepping stone toward comprehending the complexities of chemical transformations on catalytic surfaces. Specific questions of interest include determining the absolute dissociative sticking probability measured at the zero coverage limit (S_0), understanding its dependence on the energy of the incident reactant molecules (translational, rotational, and vibrational), and determining the magnitude of the activation barrier. Such studies provide an in-depth understanding of the nature of the dissociation step and valuable experimental benchmarks for theoretical and computational studies.

CO_2 dissociation on Cu surfaces is one such model system that has received extensive attention due to its relevance in the catalytic conversion of CO_2 to methanol.[1–3] This process has been proposed as one of the strategies to reduce atmospheric CO_2 levels, thereby helping mitigate global warming.[4] While extensive research has been conducted on understanding the interaction of CO_2 with Cu surfaces,[5,6] a comprehensive understanding of the mechanism and factors influencing dissociation of CO_2 on Cu surfaces is still lacking. On the low-index planes of copper surfaces, CO_2 only adsorbs weakly and has a high activation barrier for dissociation, with Cu(110) being the most active.[1] Nakamura and Campbell have reported the activation energy for dissociation of CO_2 on Cu(110) to be 0.64 eV, with an initial dissociative chemisorption probability (S_0) of the order of 10^{-9} at room temperature conditions.[7] These studies were performed by exposing a clean Cu(110) single crystal to high pressure (few mbar) CO_2, and measuring the O-atom coverage (resulting from dissociation) using Auger electron spectroscopy (AES) under ultra-high vacuum (UHV) conditions. The activation energy was determined by studying the rate of O-atom coverage buildup at different temperatures. Similar conclusions have been reached by a more recent study[8] using near ambient X-ray photoelectron spectroscopy (NAXPS) combined with density functional theory (DFT) based modeling. Another study[9] using similar methods (as in the work by Nakamura and Campbell[7]) reported an activation energy of 0.96 eV for CO_2 dissociation on

Cu(100) under high-pressure conditions.

Adsorption studies of CO_2 on Cu(110) at low temperatures (45 K - 120 K) have shown no detectable CO or adsorbed oxygen species using high-resolution energy electron loss spectroscopy (HREELS) and AES,[10] indicating that CO_2 does not undergo chemisorption on low-index plane surfaces of copper. Based on temperature programmed desorption measurements after the exposure of a clean Cu(110) surface to CO_2 (leaked into the UHV chamber, 300 K, dose = 4 Langmuir(L)), Fu and Samorjai reported that no dissociation could be observed.[11] However, under similar conditions, they also reported that CO_2 readily dissociates on stepped Cu(311) and Cu(332) surfaces, forming CO and adsorbed oxygen at a dose of 4L and surface temperature of 150 K.[11] These observations are consistent with the fact that the dissociation of CO_2 on low-index planes of copper surfaces has a much higher activation barrier when compared to stepped surfaces.

Molecular beam surface scattering experiments are well-suited to study such high-barrier dissociation processes. Here the incidence energy of the molecular beam can be precisely controlled and the S_0 along with its incidence energy dependence can be studied to understand the characteristics of the reaction pathway. Interestingly, Funk and co-workers using molecular beam methods have reported[12] no evidence of dissociation of CO_2 on Cu(110) within their detection limit ($S_0 = 0.03$) even with high incidence translation energies (E_i) ranging up to 1.3 eV. This is indeed surprising as the experimentally estimated dissociation barrier was much lower at 0.64 eV.[7] Our previous work[13] using molecular beam-surface scattering resolves this apparent inconsistency revealing that the S_0 ranges from 3.9×10^{-4} to 1.8×10^{-2} within the E_i range of 0.64 eV to 1.59 eV. We also found that the S_0 at E_i = 1.59 eV, nearly the limit of what can be obtained using a room temperature nozzle, showed a strongly increasing trend with E_i, suggesting that it is still far from reaching its maximum value. Assuming a 1-dimensional (1D) potential energy surface (PES) and based on extrapolating the observed trend in the E_i dependence of S_0, the activation barrier was estimated to be of the order of 2 eV. Interestingly, recent theoretical work on the same system, based

on dynamical calculations on a high-dimensional PES, suggests that CO_2 dissociation on Cu(110) occurs via a much more complex pathway (compared to a simple 1D picture) involving multiple barriers and in an indirect manner.[14] The activation barrier was estimated to be of the order of 0.6 eV, consistent with several previous studies, but is in contrast to the conclusions from our recent molecular beam-based studies.[13] Low values of the S_0, even at E_i much larger than the estimated barrier height, were attributed to the fact that the reaction pathway is highly constrained, leading to only a small fraction of the incident molecules to dissociate.

Given this situation, a more detailed study of the dissociation of CO_2 on Cu(110) is imperative to understand the dissociation dynamics better. In particular, dependence of the S_0 on E_i needs to be understood at larger energies well beyond 2 eV, especially to check if any signs of a highly constrained reaction pathway are observed or not. In addition, examining the normal energy scaling, the effect of vibrational excitation of incident molecules, and understanding the surface temperature (T_s) dependence of the S_0 can also provide valuable information towards understanding the nature of the reaction pathway. In this work, we have studied the dissociation of CO_2 on Cu(110) surface across a wide range of E_i, ranging from 0.28 eV to 4.6 eV. We have also investigated the effect of incident angle on the S_0, to test the validity of normal energy scaling and looked into the effect of T_s on the S_0. To produce beams of CO_2 at high E_i (> 1.7 eV) a heated nozzle was employed. This also allows us to understand the role of vibrational energy of the incident CO_2 molecules in the dissociation step.

Experimental methods

A detailed description of our molecule-surface scattering apparatus has been provided in our previous work[13] and only a concise description is presented here. It consists of a source chamber and two differential pumping stages (Diff-1 and Diff-2) followed by a UHV chamber

where the Cu(110) target single crystal was placed. The Cu(110) single crystal (disk-shaped, 10 mm diameter and 2 mm thickness) is specified to be 99.9999% pure, cut within a precision of 0.1 degrees, and polished to a roughness below 10 nm (MaTeck Material Technologie and Kristalle GmbH). It was mounted on a four-axis (XYZθ) differentially pumped manipulator using 0.25 mm diameter tungsten wires.

The UHV chamber had a base pressure of 5 $\times 10^{-10}$ mbar and is equipped with a cylindrical mirror analyzer based Auger electron spectrometer (AES), a quadrupole mass spectrometer (QMS) for incident beam flux measurements and residual gas analysis. The Cu(110) surface can be heated and the surface temperature was monitored using a K-type thermocouple attached to the side of the crystal. For routine measurements, the Cu(110) surface was cleaned by ion bombardment (Ar ion at 3 keV, ion current 0.6 μA, 30 min) followed by annealing at 800 K (30 min). Surface cleanliness was checked using AES measurements.

For the molecular beam source, a pulsed solenoid valve with an opening diameter of 1 mm (Parker 009-1643-900, driver Iota One 060-0001-900) placed in the source chamber was used. In addition, we have a SiC tube (20 mm length, 1 mm inner diameter, 3 mm outer diameter, WireTrex Limited, Germany) attached to the nozzle orifice. This SiC tube when painted with a thin layer of carbon paste can be resistively heated up to 900 K with 8 watts of electrical power (SI-1). The amount of CO_2 incident on the target surface was estimated for every measurement from the partial pressure changes monitored using the QMS. The QMS was calibrated using an independently calibrated ionization gauge as a reference. Detailed calibration procedures are described in our previous work.[13] The incident beam diameter ranged from 2.2 mm to 2.6 mm (depending on the gas mixture and the nozzle temperature, T_{n}) and was estimated from the spatial distribution of the O-atom coverage measured after the CO_2 beam exposure for each experiment. The spatial distribution of the O-atom coverage was measured using a combination of surface current and AES (SI-2). This information was used to estimate the incident CO_2 flux on the target surface, which ranged from 0.05 - 0.8 ML/sec for different gas mixtures and nozzle conditions. Here 1 ML corresponds to

1.08×10^{15} atoms cm^{-2}, the surface density of Cu atoms on a flat Cu(110) surface.[15]

Preparation of molecular beam and its characterization

For producing beams of CO_2 with different E_i (0.28 eV to 1.7 eV), we employed seeded molecular beams having different concentrations of CO_2 in H_2 ranging from 30% to 0.5%, with the nozzle at 300 K. Higher E_i beyond this limit were produced by varying the nozzle temperature up to 850 K. This allowed us to produce CO_2 beams with E_i up to 4.6 eV. The backing pressure used in all these measurements was 4 bar.

Incident translation and rotation energies and their distributions were determined using spectroscopic methods in combination with our newly developed ion imaging setup. Due to the lack of availability of efficient resonance-enhanced multiphoton excitation (REMPI) schemes for CO_2, we chose to use CO as a proxy instead. These measurements were carried out under identical experimental conditions as used for CO_2. It should be noted that systematic differences in the rotational cooling of the incident beam can arise due to the larger rotation constant of CO (compared to CO_2). Hence, our inferences are valid under the assumption that small changes in the rotation state distributions will not affect the S_0 values by much.

Our findings revealed that the incident beam rotational temperature typically ranged from 10 K to 15 K for $T_n = 300$ K and increased to 55 K at $T_n = 838$ K. The spread in E_i ($\Delta E/E$, full width at half maximum), measured at different T_n ranged from 20% to 56% for 300 K to 853 K, respectively. The estimates for E_i were found to be consistent with the following relation:

$$E_i = \frac{X_{CO_2} C_{P_{CO_2}} + X_{H_2} C_{P_{H_2}}}{X_{CO_2} M_{CO_2} + X_{H_2} M_{H_2}} M_{CO_2} (T_n - T_R) \quad (1)$$

Here, X_{CO_2} and X_{H_2} represent the mole fractions of CO_2 and H_2, respectively. $C_{P_{CO_2}}$ and $C_{P_{H_2}}$ indicate the heat capacities of CO_2 and H_2, respectively. T_n corresponds to the nozzle temperature, T_R represents the rotational temperature of the molecular beam and M_{CO_2}

represents the molar mass of CO_2. A detailed characterization of the translation and rotation energy distribution of the incident beams used in this work is provided in SI-3.

The fraction of vibrationally excited CO_2 in the incident beam at high T_n was estimated assuming minimal vibrational relaxation in the nozzle. A qualitative confirmation of the same was also obtained using the 3+1 REMPI scheme for CO_2 at 330 nm.[16] Although this scheme is inefficient, it was good enough to observe a systematic increase in the bending (010) state population (relative to the ground state) with increasing T_n (SI-4). Based on these measurements we estimate that 26% population is in the excited bending state (010) and 8.5% is in the (020) state, at T_n= 853 K. The estimated relative uncertainty in S_0 is about 20% (1σ) and arises mainly from the uncertainties in the incidence beam flux and O-atom coverage measurements.

Results

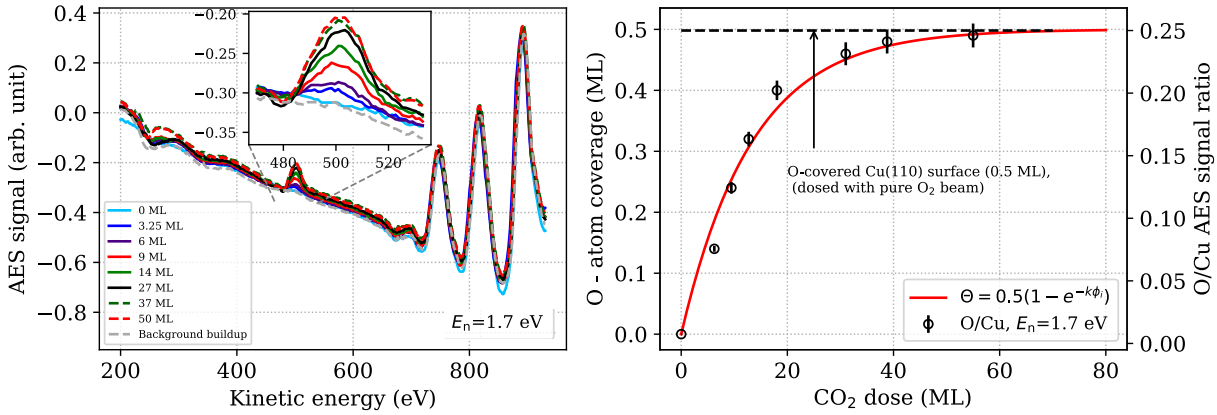

Figure 1: (left) Auger electron spectra of the Cu(110) surface measured at different incident dose of CO_2 at $E_n = 1.7$ eV. Background buildup of O-atom coverage was measured after the last measurement, at a different position on the surface which was not exposed to incident CO_2 beam. (right) A plot of O-atom coverage build-up with increasing CO_2 dose obtained from the AES measurements shown in the left panel. The coverage estimation was made using the AES peak ratio of O(503 eV) and Cu(776 eV). Red curve is the best fit using a first-order kinetics model. The dashed black line shows the saturation coverage obtained for dissociative chemisorption of O_2 on the same surface (measured independently).

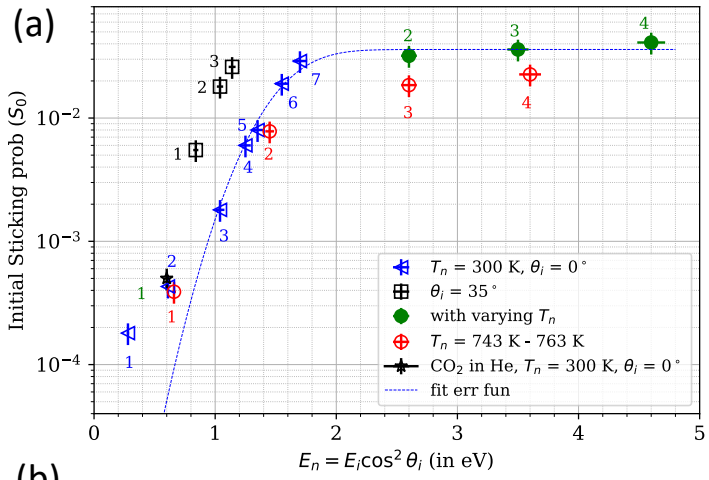

(b)

Measurements		(% CO_2 in H_2)	T_n (K)	θ_i (^{0})	E_n (eV)	$\frac{\Delta E}{E}$ (%)	S_0
	1	30	300	0	0.28	20	1.8×10^{-4}
	2	10	300	0	0.6	20	4.8×10^{-4}
	3	3.8	300	0	1.04	20	1.9×10^{-3}
	4	2.4	300	0	1.25	20	6.1×10^{-3}
	5	1.8	300	0	1.35	20	8.1×10^{-3}
	6	1	300	0	1.55	20	1.5×10^{-3}
	7	0.5	300	0	1.7	20	2.9×10^{-2}
	1	30	473	0	0.4	35	2.5×10^{-4}
	2	0.5	463	0	2.6	34	3.2×10^{-2}
	3	0.5	623	0	3.4	43	3.5×10^{-2}
	4	0.5	838	0	4.6	56	4.1×10^{-2}
	1	30	750	0	0.66	51	3.9×10^{-2}
	2	10	745	0	1.45	51	7.9×10^{-3}
	3	3.8	763	0	2.6	52	1.8×10^{-2}
	4	1	743	0	3.6	51	2.3×10^{-2}
	1	2.4	300	35	0.84	20	5.5×10^{-3}
	2	1	300	35	1.04	20	1.8×10^{-3}
	3	0.5	300	35	1.14	20	2.6×10^{-2}
		1 (in He)	300	0	0.6	20	4.9×10^{-4}

Figure 2: (a) A plot of the S_0 versus normal component incident energy of CO_2 on Cu(110). Blue triangles indicate measurements at normal incidence with T_n = 300 K. Black squares correspond to measurements at an incidence angle of 35° with T_n = 300 K. Red open circles represent measurements at elevated nozzle temperatures between 743 K and 763 K. Filled green circles denote measurements performed over a range of nozzle temperatures (473 K to 838 K) and for CO_2 concentrations of 30% and 0.5% in H_2. The dashed blue curve is a fit using a S-shaped function. The numbers associated with each point are labels for identifying the experimental parameters and incident beam characteristics, described in panel (b). Note that the T_n was maintained within ± 5 K of the aforementioned values across all measurements. The experimental error in the E_i determination typically ranged from 2% to 8% (SI-3) when using the spatial ion imaging technique with CO as a proxy.

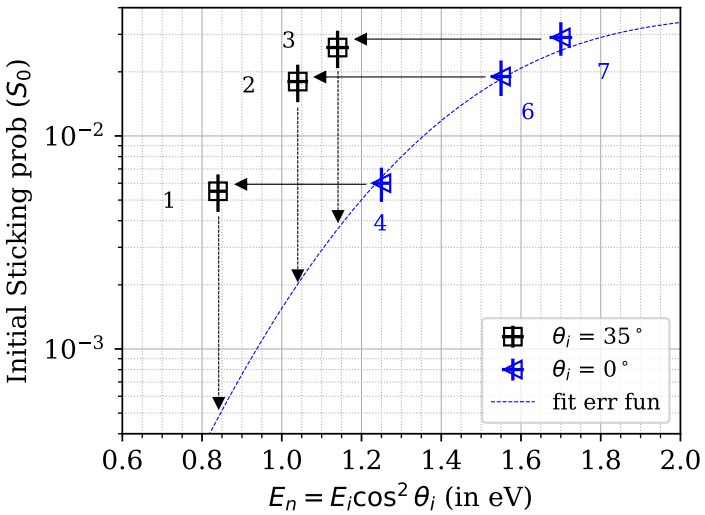

Figure 3: A comparison of the S_0 observed at a $\theta_\mathrm{i} = 35°$ (black open squares) and $\theta_\mathrm{i} = 0°$ (blue open triangles) at the same E_i. Horizontal arrows indicate a change in E_n, and the heads of the vertical arrows represent the expected S_0 values if normal energy scaling was followed. The blue dashed line is a fit (same as in Figure 2(a)) using an S-shaped curve and the numbers correspond to the same labeling scheme as in Figure 2 .

Initial sticking probabilities for dissociative chemisorption of CO_2 on Cu(110) were determined by measuring O-atom coverage (measured using AES) as a function of incident CO_2 dose. Figure 1 (left) shows the AES signal measured at different incident CO_2 doses ranging from 0 to 60 monolayers (ML), with $E_\mathrm{i} = 1.7$ eV and incidence angle (θ_i) = 0°. A clear trend of increasing surface O-atom coverage with CO_2 dose is seen. Quantitative analysis of this trend was obtained by analyzing the ratio of oxygen to Cu peak-to-peak signal (background subtracted) as a function of incident CO_2 dose (Figure 1, right). The O/Cu AES signal ratio reached a value of 0.24 ± 0.01 at saturation coverage. To obtain the corresponding O-atom coverage in monolayers, we independently measured the dissociative chemisorption of O_2 on this surface for calibration. The saturation O/Cu AES signal ratio obtained in both the cases (O_2 and CO_2 dosing) were observed to be the same (black dashed line in Figure 1, right panel). Given that it is well-established from several previous studies that O_2 exposure leads to a saturation O-atom coverage of 0.5 ML, owing to a (2×1) overlayer structure,[17–21] we conclude that the CO_2 dissociation leads to a saturation O-atom coverage

of 0.5 ML as well. This also rules out the presence of any unwanted clean-up reactions affecting our measurements, even when using H_2 seeded beams along with a heated nozzle.[22] It is worth pointing out that at E_i higher than 3 eV we see an increased saturation coverage (0.66 ML). While this point is discussed in more detail later, it should be noted that this does not affect the O-atom coverage estimation presented here. The surface O-atom coverage build-up as a function of the incident CO_2 dose was fitted with a simple first-order kinetics model: $\Theta = \Theta_{sat}(1 - e^{-k\phi_i})$. Here, ϕ_i corresponds to the incident CO_2 dose, and the value of saturation coverage (Θ_{sat}) is set to 0.5 ML. The slope of this function in the zero coverage limit ($0.5 \times k$) gives the initial dissociative sticking probability of CO_2 on Cu(110).

Incident translational energy and impact angle dependence of the initial sticking probability

The S_0 values of CO_2 on the Cu(110) surface obtained under different experimental conditions are depicted in Figure 2(a). Blue triangles represent S_0 values measured at normal incidence ($\theta_i = 0°$) and $T_n = 300$ K. Green-filled circles depict the measurements carried out using a heated nozzle at different temperatures. The red circles (hollow) indicate measurements at nozzle temperatures ranging from 743 K to 763 K, at normal incidence for different gas mixtures. Black squares depict measurements at $\theta_i = 35°$ for three different E_i of 1.7 eV, 1.55 eV, and 1.25 eV, corresponding to E_n of 1.14 eV, 1.04 eV, and 0.84 eV, respectively. The blue dashed curve represents an empirical fit in the form of an S-shaped curve, which is discussed later. A detailed description of the molecular beam characteristics for each of the measurements is shown in Figure 2(b). The values of S_0 obtained in these sets of measurements are consistent with the previously reported values[13] (SI-5).

These results clearly show that with increasing E_n from 0.28 to 4.6 eV, S_0 increases from 1.9×10^{-4} to 4.1×10^{-2}. Importantly, S_0 increases rapidly with E_i up to 2 eV and only very slowly beyond this. A comparison of the measurements performed at $\theta_i = 35°$ and $0°$ are shown in detail in Figure 3. The observed S_0 (for a given E_i) remains largely unchanged with

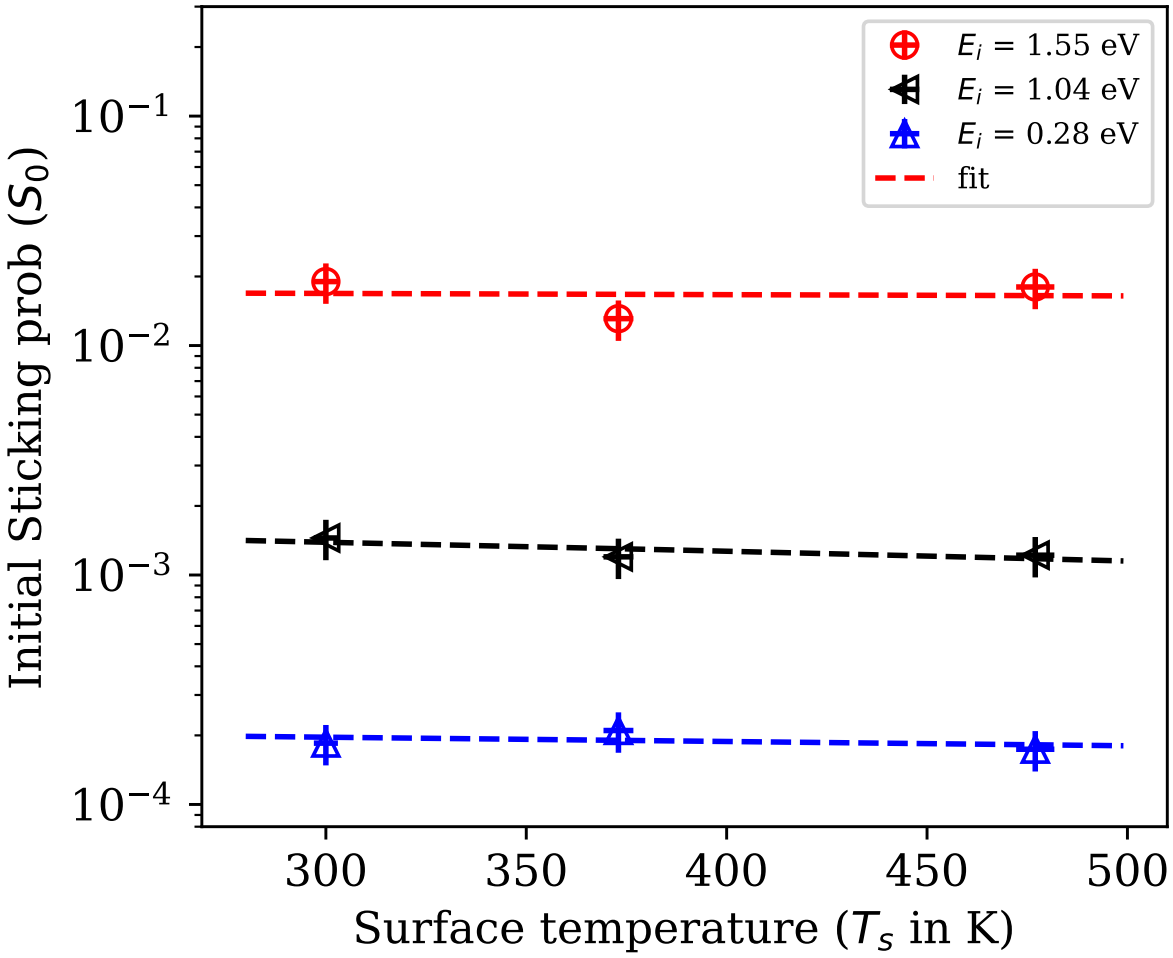

Figure 4: S_0 obtained for different surface temperatures at E_i = 0.28 eV, 1.04 eV, and 1.55 eV, T_n = 300 K).

the incidence angle. These observations show a large deviation from the expected values if the normal energy scaling was valid (depicted by the tip of black vertical arrows, Figure 3) and are consistent with total energy scaling. We also point out that in our previous study[13] on the same system, we could not firmly establish this aspect as the largest incident angle used was only $\theta_\mathrm{i} = 19°$ due to experimental design limitations. The present version of the experimental setup allows for larger incidence angles and enables us to see these changes more clearly.

S_0 values obtained with higher T_n (743 K - 763 K) are shown in red open circles in

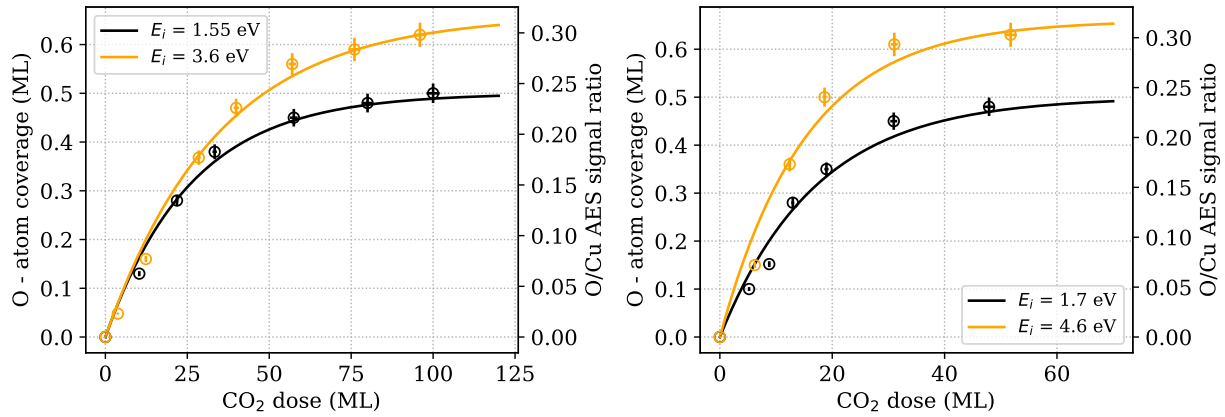

Figure 5: Comparing the O-atom coverage as a function of incident CO_2 dose at low and higher E_i. Measurements at E_i = 1.55 eV and 3.6 eV (left), and 1.7 eV and 4.6 eV (right). These results correspond to point #6 (blue triangle), point #4 (red hollow circle), point #7 (blue triangle), and point #4 (green filled circle) shown in Figure 2(a), respectively. In both sets of measurements, the saturation coverage at higher incident energy is larger. Note that the data presented at 1.7 eV (right panel) is from an independent measurement (under similar conditions) compared to that shown in Figure 1.

Figure 2(a). A comparison with S_0 values at similar E_i, but at lower T_n (obtained using a more dilute mixture of CO_2 in H_2), a slight decrease was observed. Qualitatively speaking, at E_i larger than 2 eV, this decrease is consistent with that expected from broadened E_i distribution of the incident beam at higher nozzle temperatures, especially when combined with the fact that the S_0 only increases very slowly at energies larger than 2 eV. However, at lower E_i a corresponding increase is not observed, indicating that the spread in E_i is not the sole contributing factor here (SI-6). Given the limitations of the present set of experiments where the E_i has been estimated indirectly, the spread in E_i, rotational and vibrational state distribution can not be controlled independently, and that we have only a few such measurements, we are unable to conclusively understand this trend. A direct E_i measurement of CO_2 especially over the entire temporal incidence beam profile can possibly help in understanding this issue better. Nonetheless, this observation does rule out any significant enhancement in S_0 caused by the vibrationally excited incident CO_2 molecules under our experimental conditions. This is important as the low-lying bending mode is expected to be populated significantly at higher T_n.

The high nozzle temperatures used in combination with CO_2 seeded in H_2 raises a potential concern about the presence of Reverse Water-Gas Shift (RWGS) reaction, which can adversely impact our measurements.[23] Specifically, there is a possibility that the RWGS reaction could produce CO and H_2O, which might interfere with our S_0 measurements. In particular, the dissociative chemisorption of H_2O can also lead to oxygen atom buildup on the Cu(110) surface in addition to CO_2 dissociation. To assess this situation better, we used a Quadrupole Mass Spectrometer (QMS) to monitor any increase in CO levels with increasing T_n. As the CO signal on QMS also results from the residual gases in the UHV chamber and the electron impact fragmentation of CO_2 in the QMS, the ratio of CO to CO_2 partial pressure was chosen as a measure for detecting small changes in CO levels as T_n was varied. Our detection sensitivity, capable of discerning changes in the CO to CO_2 partial pressure ratio as small as 4%, revealed no significant variation in this ratio, indicating that CO production via RWGS was minimal even at the highest T_n used in this work. Further confirmation comes from the measurement of S_0 at $T_n = 750$ K for a mixture containing 30% CO_2 in H_2 (Figure 2(a), red hollow circle #1, $E_i = 0.66$ eV). Here, any additional O-atom coverage buildup due to RWGS is expected to show up as an increase in the estimated S_0. However, the observed reaction probability is 3.9×10^{-4}, consistent with the overall trend showing no anomalous increase. Additionally, the measurement with a beam of 1% CO_2 in He with $E_i = 0.6$ eV (black star, Figure 2(a)), where no RWGS reaction is possible, is also consistent with that observed at similar E_i using H_2 seeded beam. Based on these considerations, we rule out any overestimation of S_0 caused by RWGS, despite using the heated nozzle in our measurements.

The S_0 measured at different T_s of 300 K, 380 K, and 480 K are shown in Figure 4. These measurements were carried out for three different E_i of 0.28 eV, 1.04 eV, and 1.55 eV at normal incidence. No measurable change in the S_0 was observed with increasing surface temperature for all three energies. This clearly shows that within 300 K to 480 K, surface temperature does not play a significant role in the dissociative chemisorption of

CO_2. Another interesting feature observed is that saturation O-atom coverage seen in our measurements increases from 0.5 ML to 0.66 ML for E_i greater than 3 eV (Figure 5). This suggests that at higher E_i new reaction sites become accessible.

Discussion

Dependence of the S_0 on E_i at normal incidence can be divided into two characteristic regions. In the first region below 2 eV, S_0 increases by more than 150 times as the E_i changes from 0.28 eV to 2 eV. This indicates a translationally activated process with a high activation barrier. In the second region of 2 eV to 4.6 eV, S_0 increases by a factor of less than 1.5, and is 4.1×10^{-2} at 4.6 eV. The values of the S_0 being low at large E_i (much greater than the estimated barrier) is an indication of a severely constrained reaction pathway. Similar characteristics have been reported in other cases previously, for example, the well-studied N_2/Ru(0001) system. Here too the S_0 increases very slowly with E_i, with much larger than the activation barrier.[24] Based on simulations over a six-dimensional PES[25] it was found that increased surface corrugation and anisotropy near the minimum energy pathway creates a narrow bottleneck, thereby explaining the low reactivity, even at much higher energies than the dissociation barrier. A similar situation could be prevailing in this case as well. The slow increase in the S_0 even at E_i well above 2 eV is consistent with a highly constrained reaction pathway, allowing only a small fraction of configurations to overcome the barrier, regardless of the available incident energy. Similar conclusions have been drawn from recent work by Yin and coworkers[14] based on simulations for the CO_2/Cu(110) system on a multidimensional PES. Although, at the moment results from simulations are only available up to an E_i of 2 eV, it will be interesting to look into the reaction probabilities predicted by extending this work to higher E_i.

Another significant finding arising from this work is that the dissociative chemisorption probability of CO_2 on Cu(110) is largely independent of the incidence angle and follows total

energy scaling, rather than normal energy scaling (Figure 3). In many cases of molecule-surface collisions, where the interaction PES exhibits low corrugation, the parallel component of the incident momentum does not get exchanged and largely behaves like a spectator mode. This leads to the so called normal energy scaling, where the S_0 solely depends on E_n (and not on E_i).[26–30] On the other hand, if the molecule-surface interaction potential is corrugated or is highly anisotropic, then a significant exchange among the perpendicular and parallel components of incident momenta can occur, ultimately leading to deviation from normal energy scaling. Similar characteristics have been reported previously for the physisorption dynamics of CO_2 on Cu(110),[5] studied up to an E_i of 1.3 eV. Here too the physisorption probability was reported to follow total energy scaling. Since we have measured CO_2 dissociation probability at much higher incident energies, it is reasonable to conclude that the incident molecules penetrate the surface electron density sufficiently and encounter a significant amount of corrugation. This combined with the anisotropic nature of the PES can give rise to the total energy scaling behavior, as observed in the present case. Further experiments, especially looking into the inelastic scattering and energy transfer, are likely to shed more light on this aspect. In particular, broadening of the angular distribution as a function of incident energy caused by large corrugation is expected.

Another noteworthy point is that incident beams at a high nozzle temperature, having a higher fraction of vibrationally excited CO_2, especially in the low-lying bending modes, do not show a measurable increase in S_0 for the same E_i (red open circles, Figure 2(a), T_n = 743 - 763 K). The total bending mode population at T_n = 750 K is estimated to be 34% (26.5% in (010) and 7.5% in (020) state, see SI-4). This estimate allows us to put an upper limit to the relative efficiency of vibrational and translational energy in overcoming the reaction barrier, often described in terms of vibrational efficacy.[31,32] In particular, S_0 measurements at nearly the same incident energy but at different nozzle temperatures help us understand this aspect better. Consider the measurements at $E_i \sim 0.6$ eV with T_n = 300 K and 750 K (Figure 2(a), blue triangle, point #2 and hollow red circle, point #1), and measurements

at $E_i \sim 1.4$ eV at $T_n = 300$ K and 745 K (Figure 2(a), blue triangle point #5 and hollow red circle point #2). At 750 K, the mean vibrational energy of the incident CO_2 beam is 0.08 eV (assuming no vibrational relaxation in the expansion process). For the same energy provided in the form of translational energy, S_0 increases approximately by a factor of two. If we assume the vibrational efficacy to be 1, we would expect S_0 to increase by a factor of two, which would be clearly discernible in our measurements. However, our results clearly show that there is no such increase. Based on the uncertainty in S_0 estimation, we conclude that the upper limit of vibrational efficacy for this system is 0.25.

This is rather surprising since several studies have indicated that the transition state has a bent configuration in dissociative chemisorption of CO_2 on various metal surfaces.[8,33,34] Interestingly, for the closely related system of CO_2 dissociation on Ni(100), a factor of 2-10 increase in S_0 was observed at a 1000 K nozzle temperature compared to 300 K.[30] Similarly, a recent study of CO_2 on an H-covered Cu(111) and Cu(100) surface reported a vibrational efficacy of 8-9 for the hydrogen pickup reaction through the Eley-Rideal mechanism.[35] A recent study of CO_2 dissociation dynamics on Cu(110) using multidimensional PES also suggests that excitation of bending vibrational mode enhances the reaction probabilities.[14] These findings are in contrast with our observation where no vibration enhancement is seen.

We attribute this lack of vibrational enhancement to be resulting from the fact that the overall vibrational energy of the incident beam is still much smaller compared to the dissociation barrier. On the other hand, numerous previous studies where significant vibrational enhancement has been reported, are systems where the vibrational energy is comparable to the dissociation barrier height.[30,31] Another point that should be noted is that previous experimental work, such as HREELS studies of CO_2 adsorbed on low-index planes of Cu, have also shown no evidence of chemisorption or bent CO_2 state on Cu(110) surface.[10] However, a chemisorption state was observed for high-index planes of copper surfaces.[6] The absence of any role for vibrational energy in our measurements suggests that the bent configuration as a transition state is unlikely for low-index planes such as Cu(110).

We also explored the role of surface temperature on the dissociation probabilities. It is well understood that in direct dissociation processes, surface temperature has a minimal effect. However, in some systems, surface temperature can influence the reaction barrier and dissociation dynamics.[29] For example, in the dissociative chemisorption of CH_4 on a Pt(110)-(1×2) surface, increasing T_s from 400 K to 600 K reduced the dissociation barrier height by 0.09 ± 0.02 eV, with an estimated surface temperature efficacy of 5.1.[28] Motivated by such findings, we sought to understand the role of T_s in the current system. Here, the temperature range was chosen based on previous literature, which indicates that prolonged annealing above 500 K can lead to the incorporation of oxygen atoms into the surface or the formation of a supergrating-like structure.[36,37] To avoid such complications, we maintained T_s well below 500 K. The measurements were performed at three translational energies: 0.28 eV, 1.04 eV, and 1.55 eV. Our studies show no significant effect of T_s on S_0, consistent with a direct dissociation process rather than a precursor-mediated one. We also conclude that the thermal energy of the surface is too low compared to the barrier height, and consequently no significant influence on the S_0 is seen.

With the absence of a notable T_s effect on dissociation, we aimed to determine the barrier height and its distribution for the direct dissociation process (assuming a simplified 1D PES). Since both parallel and perpendicular momentum contribute similarly to overcoming the dissociation barrier, it is reasonable to assume that the barrier height distribution is consistent across all angles of incidence. Therefore, we used the measurements at normal incidence and nozzle temperature of 300 K to fit an S-shaped function for determining the barrier height and its distribution. Barrier height distribution is a convolution of various parameters, including beam energy distribution, surface temperature, the vibrational energy of molecules, the orientation of molecules in the molecular beam, and impact sites. Given our findings that surface temperature and vibrational energy have minimal influence on dissociation probability, the remaining parameters significantly contribute to the barrier height distribution. Knowing the energy spread of our incident beam, which ranged from

20% to 55% for T_n varying from 300 K to 850 K, respectively (see SI-3), we can infer the contribution of orientation and impact sites on barrier height distribution. From the S-shaped fitting function, we obtained the parameters: $A = 0.04$, $E_0 = 1.6$ eV, and $W_0 = 0.4$ eV. After accounting for the energy spread in the molecular beam, the effective barrier width W_0 was determined to be 0.3 eV (see SI-7). To further understand the individual contribution of orientation and impact sites on the S_0, it will be interesting to look into the results from simulations.

The last point to be discussed is the increase in saturation coverage (from 0.5 to 0.66 ML), observed at E_i greater than 3 eV. Since this enhanced saturation coverage is only seen for higher E_i where a heated nozzle was employed, it is important to first understand if RWGS or increased ro-vibrational excitation has any role to play here. To understand this better, we turn our attention towards S_0 measurements using a 30% CO_2 in H_2 mixture at T_n = 750 K, corresponding to E_i= 0.66 eV (point #1, red hollow circle in Figure 2(a)). Here too we observed that the O-atom coverage saturated at 0.5 ML. Further, no appreciable change in the S_0 was observed compared to the overall trend at T_n = 300 K. Based on these observations we rule out any role of increased ro-vibrational excitation (in the incident beam) leading to an increased saturation coverage. As also discussed earlier, this rules out the presence of RWGS (in the heated nozzle) and consequently its contribution towards the increased saturation coverage.

To understand this issue better, we turn our attention to the dissociative chemisorption of O_2 on Cu(110), which is a well-studied system.[6,38] Previous literature firmly establishes that after dissociation, the O-atom coverage saturates at 0.5 ML, forming a (2×1) overlayer.[36,37] It is also known that prolonged exposure to O_2 (10^5 Langmuir) leads to the formation of a new (6×2) O-Cu structure with 0.66 ML O-atom coverage,[37] similar to what we see at higher incident energies. A similar situation has also been reported for the N_2/W(110) system.[39] In this work, it was reported that the saturation coverage is 0.25 ML at an energy of 0.1 to 1 eV. At higher incidence kinetic energies (2 eV), this saturation coverage increases to around

0.5 ML. Low-energy electron diffraction (LEED) studies[39] revealed a p(2×2) structure at 0.25 ML coverage and c(4×2) structure at 0.5 ML coverage. In light of the above points, we attribute the increased surface coverage at higher E_i to specific surface sites having a higher activation barrier for dissociation becoming accessible at E_i beyond 3 eV.

Summary and Concluding Remarks

In this work, we have studied the dissociative chemisorption of CO_2 on a Cu(110) using a heated nozzle with E_i up to 4.6 eV. Our findings reveal that the S_0 increases very slowly with increasing E_i beyond 2 eV. Additionally, the E_i dependence of S_0 is consistent with total energy scaling, indicating a significant corrugation in the interaction potential. Another finding of this work is that vibrational energy (especially the bending mode) does not play a significant role in the dissociation probability, with an upper limit of vibrational efficacy estimated to be 0.25. These observations are consistent with previous UHV adsorption studies that reported no chemisorption state of CO_2 on the Cu(110) surface. Furthermore, an increase in the saturation coverage from 0.5 ML to 0.66 ML at E_i higher than 3 eV shows that new surface sites with higher activation barriers become accessible at higher E_i. Importantly, the S_0 values even at large E_i are of the order of 10^{-2} and only increase slowly. These observations are consistent with a highly constrained reaction pathway where only a small fraction of incident molecules can cross the dissociation barrier. For obtaining deeper insights into the dissociation dynamics it will be interesting to look into the dissociation process with state-selective preparation of incident CO_2, as demonstrated recently.[40] This will help in understanding the role of vibration excitation and possibly the effect of alignment of the incident CO_2 on the S_0, shedding more light on the configurations that are more favorable for barrier crossing.

Acknowledgement

We acknowledge the support of intramural funds at TIFR-Hyderabad provided by the Department of Atomic Energy, Government of India, under Project Identification No. RTI 4007 and Scientific and Engineering Research Board, Department of Science and Technology, India (Grant number. CRG/2022/002943). We thank Minali for her help with the design and testing of the heated nozzle. Helpful discussions on the practical aspects of ion imaging with Theofanis Kitsopoulos are acknowledged. We also thank M. Krishnamurthy and Ram Gopal for providing the MCP detector.

Supporting Information Available

- SI-1: Heated nozzle design and operation
- SI-2: Molecular beam profile at the Cu(110) surface
- SI-3: Molecular beam characterization
- SI-4: Using the hot nozzle to understand the role of vibrational excitation in CO_2 dissociation
- SI-5: Comparison with previous work
- SI-6: Effect of broad energy distribution on initial reaction probability
- SI-7: Barrier height distribution measurement

Author contributions

SKS and PRS conceived and designed the study. SKS performed the measurements and analyzed the results with inputs from PRS. SKS and PRS discussed the results and prepared the manuscript.

References

(1) Yoshihara, J.; Campbell, C. T. Methanol Synthesis and Reverse Water–Gas Shift Kinetics over Cu(110) Model Catalysts: Structural Sensitivity. *Journal of Catalysis* **1996**, *161*, 776–782.

(2) Jiang, X.; Nie, X.; Guo, X.; Song, C.; Chen, J. G. Recent Advances in Carbon Dioxide Hydrogenation to Methanol via Heterogeneous Catalysis. *Chemical Reviews* **2020**, *120*, 7984–8034.

(3) Waugh, K. Methanol synthesis. *Catalysis Today* **1992**, *15*, 51–75.

(4) Olah, G. A. Towards Oil Independence Through Renewable Methanol Chemistry. *Angewandte Chemie International Edition* **2013**, *52*, 104–107.

(5) Funk, S.; Hokkanen, B.; Wang, J.; Burghaus, U.; Bozzolo, G.; Garcés, J. Adsorption dynamics of CO_2 on Cu(110): A molecular beam study. *Surface Science* **2006**, *600*, 583–590.

(6) Fu, S. S.; Somorjai, G. A. Interactions of O_2, CO, CO_2, and D_2 with the stepped Cu(311) crystal face: Comparison to Cu(110). *Surface Science* **1992**, *262*, 68–76.

(7) Nakamura, J.; Rodriguez, J. A.; Campbell, C. T. Does CO_2 dissociatively adsorb on Cu surfaces? *Journal of Physics: Condensed Matter* **1989**, *1*, SB149–SB160.

(8) Yang, T.; Gu, T.; Han, Y.; Wang, W.; Yu, Y.; Zang, Y.; Zhang, H.; Mao, B.; Li, Y.; Yang, B.; Liu, Z. Surface Orientation and Pressure Dependence of CO_2 Activation on Cu Surfaces. *The Journal of Physical Chemistry C* **2020**, *124*, 27511–27518.

(9) Rasmussen, P. B.; Taylor, P. A.; Chorkendorff, I. The interaction of carbon dioxide with Cu(100). *Surface Science* **1992**, *269*, 352–359.

(10) Ernst, K. H.; Schlatterbeck, D.; Christmann, K. Adsorption of carbon dioxide on Cu(110) and on hydrogen and oxygen covered Cu(110) surfaces. *Physical Chemistry Chemical Physics* **1999**, *1*, 4105–4112.

(11) Fu, S. S.; Somorjai, G. A. Interactions of O_2, CO, CO_2, and D_2 with the stepped Cu (311) crystal face: Comparison to Cu(110). *Surface Science* **1992**, *262*, 68–76.

(12) Funk, S.; Hokkanen, B.; Wang, J.; Burghaus, U.; Bozzolo, G.; Garcés, J. E. Adsorption dynamics of CO_2 on Cu(110): A molecular beam study. *Surface Science* **2006**, *600*, 583–590.

(13) Singh, S. K.; Shirhatti, P. R. The curious case of CO_2 dissociation on Cu(110). *The Journal of Chemical Physics* **2024**, *160*.

(14) Yin, R.; Guo, H. Multidimensional Dynamics of CO_2 Dissociative Chemisorption on Cu(110). *The Journal of Physical Chemistry C* **2024**,

(15) Zhai, R.-S.; Chan, Y. L.; Chuang, P.; Hsu, C.-K.; Mukherjee, M.; Chuang, T. J.; Klauser, R. Chemisorption and Reaction Characteristics of Methyl Radicals on Cu(110). *Langmuir* **2004**, *20*, 3623–3631.

(16) Taylor, D. P.; Johnson, P. M. Resonance enhanced multiphoton ionization photoelectron spectra of CO_2. III. Autoionization dominates direct ionization. *The Journal of chemical physics* **1993**, *98*, 1810–1816.

(17) Ertl, G. Untersuchung von oberflächenreaktionen mittels beugung langsamer elektronen (LEED). *Surface Science* **1967**, *6*, 208–232.

(18) Gruzalski, G.; Zehner, D.; Wendelken, J. Two adsorbate densities for Cu(110)c(6×2)-O. *Surface Science Letters* **1984**, *147*, L623–L629.

(19) Gruzalski, G.; Zehner, D.; Wendelken, J. An XPS study of oxygen adsorption on Cu(110). *Surface Science* **1985**, *159*, 353–368.

(20) Jensen, F.; Besenbacher, F.; Laegsgaard, E.; Stensgaard, I. Surface reconstruction of Cu(110) induced by oxygen chemisorption. *Physical Review B* **1990**, *41*, 10233–10236.

(21) Baddorf, A. P.; Wendelken, J. F. High coverages of oxygen on Cu(110) investigated with XPS, LEED, and HREELS. *Surface Science* **1991**, *256*, 264–271.

(22) Hayden, B.; Lamont, C. Dissociative hydrogen adsorption and its reaction with oxygen on Cu(110). *Journal of Physics: Condensed Matter* **1989**, *1*, SB33.

(23) Thompson, R. S.; Langlois, G. G.; Li, W.; Brann, M. R.; Sibener, S. Reverse water-gas shift chemistry inside a supersonic molecular beam nozzle. *Applied Surface Science* **2020**, *515*, 145985.

(24) Diekhöner, L.; Mortensen, H.; Baurichter, A.; Jensen, E.; Petrunin, V. V.; Luntz, A. C. N_2 dissociative adsorption on Ru(0001): The role of energy loss. *The Journal of Chemical Physics* **2001**, *115*, 9028–9035.

(25) Díaz, C.; Vincent, J.; Krishnamohan, G.; Olsen, R.; Kroes, G.; Honkala, K.; Nørskov, J. K. Reactive and nonreactive scattering of N_2 from Ru(0001): A six-dimensional adiabatic study. *The Journal of chemical physics* **2006**, *125*.

(26) Campbell, J. M.; Domagala, M. E.; Campbell, C. T. Energy requirements for the dissociative adsorption of hydrogen on Cu(110). *Journal of Vacuum Science & Technology A: Vacuum, Surfaces, and Films* **1991**, *9*, 1693–1697.

(27) Luntz, A.; Brown, J.; Williams, M. Molecular beam studies of H_2 and D_2 dissociative chemisorption on Pt(111). *The Journal of chemical physics* **1990**, *93*, 5240–5246.

(28) Bisson, R.; Sacchi, M.; Beck, R. D. State-resolved reactivity of CH_4 on Pt(110)-(1$\times$ 2): The role of surface orientation and impact site. *The Journal of chemical physics* **2010**, *132*.

(29) Killelea, D.; Campbell, V.; Shuman, N.; Smith, R.; Utz, A. Surface temperature dependence of methane activation on Ni(111). *The Journal of Physical Chemistry C* **2009**, *113*, 20618–20622.

(30) D'Evelyn, M.; Hamza, A.; Gdowski, G.; Madix, R. Dynamics of the dissociative adsorption of CO_2 on Ni(100). *Surface Science* **1986**, *167*, 451–473.

(31) Beck, R. D.; Maroni, P.; Papageorgopoulos, D. C.; Dang, T. T.; Schmid, M. P.; Rizzo, T. R. Vibrational mode-specific reaction of methane on a nickel surface. *Science* **2003**, *302*, 98–100.

(32) Juurlink, L.; Killelea, D.; Utz, A. State-resolved probes of methane dissociation dynamics. *Progress in Surface Science* **2009**, *84*, 69–134.

(33) Freund, H.-J.; Roberts, M. Surface chemistry of carbon dioxide. *Surface Science Reports* **1996**, *25*, 225–273.

(34) Hagman, B.; Posada-Borbón, A.; Schaefer, A.; Shipilin, M.; Zhang, C.; Merte, L. R.; Hellman, A.; Lundgren, E.; Grönbeck, H.; Gustafson, J. Steps Control the Dissociation of CO_2 on Cu(100). *Journal of the American Chemical Society* **2018**, *140*, 12974–12979.

(35) Quan, J.; Muttaqien, F.; Kondo, T.; Kozarashi, T.; Mogi, T.; Imabayashi, T.; Hamamoto, Y.; Inagaki, K.; Hamada, I.; Morikawa, Y.; Nakamura, J. Vibration-driven reaction of CO_2 on Cu surfaces via Eley–Rideal-type mechanism. *Nature Chemistry* **2019**, *11*, 722–729.

(36) Kern, K.; Niehus, H.; Schatz, A.; Zeppenfeld, P.; Goerge, J.; Comsa, G. Long-range spatial self-organization in the adsorbate-induced restructuring of surfaces: Cu(100)-(2× 1) O. *Physical review letters* **1991**, *67*, 855.

(37) Simmons, G. W.; Mitchell, D. F.; Lawless, K. R. LEED and HEED studies of the

interaction of oxygen with single crystal surfaces of copper. *Surface Science* **1967**, *8*, 130–164.

(38) Nesbitt, A.; Lewin, A. K.; Hodgson, A. Adsorption of oxygen on Cu(110). *Journal of Physics: Condensed Matter* **1991**, *3*, S71–S76.

(39) Pfnür, H.; Rettner, C.; Lee, J.; Madix, R.; Auerbach, D. Dynamics of the activated dissociative chemisorption of N_2 on W(110): A molecular beam study. *The Journal of chemical physics* **1986**, *85*, 7452–7466.

(40) Jansen, C.; Juurlink, L. B.; van Lent, R.; Chadwick, H. A state-selected continuous wave laser excitation method for determining CO_2's rotational state distribution in a supersonic molecular beam. *Review of Scientific Instruments* **2024**, *95*.

TOC Graphic